284 *Inorg. Chem.* **1992**, *31*, 284-289

Contribution from the Laboratoire de Chimie de Coordination du CNRS, UPR 8241
Liée par Conventions à l'Université Paul Sabatier et à l'Institut Polytechnique de Toulouse,
205 Route de Narbonne, 31077 Toulouse Cedex, France

Intermolecular versus Intramolecular Exchange Interactions. Magnetic Properties of (Tetraacetylethanato(2–))bis((*N*,*N*,*N'*,*N'*-tetramethylethylenediamine)copper(II)) Diperchlorate Hydrate (I) and of (Tetraacetylethanato(2–))bis((*N*,*N*,*N'*,*N'*-tetramethylethylenediamine)copper(II)) Bis(tetraphenylborate) Hydrate (II). Crystal and Molecular Structure of I

Jean-Pierre Costes,* Françoise Dahan, and Jean-Pierre Laurent

Received April 18, 1991

The crystal structure of (tetraacetylethanato(2–))bis((*N*,*N*,*N'*,*N'*-tetramethylethylenediamine)copper(II))diperchlorate hydrate, $[(\text{TmenCu})_2\text{Tae}(\text{ClO}_4)_2{\cdot}\text{H}_2\text{O}]$ (I) has been determined. This compound belongs to the monoclinic space group $P2_1/c$ with a = 15.598 (2) Å, b = 8.748 (1) Å, c = 26.508 (3) Å, β = 106.22 (1)°, and Z = 4. In this binuclear complex, the two copper atoms are not equivalent for the first one is in a (4 + 1) surrounding while the other one seemingly adopts a (4 + 1 + 1) coordination. The apical positions around these copper atoms are occupied by oxygen atoms of perchlorate anions or of a water molecule. The dihedral angle between the planes defined by the four identical equatorial donor atoms (N_2O_2) around each copper atom equals 77.0°. The magnetic properties (static susceptibility and EPR spectroscopy) have been determined for this complex, its homologue $[(\text{TmenCu})_2\text{Tae}{\cdot}\text{H}_2\text{O}](\text{BPh}_4)_2$ (II), and their mononuclear counterpart $[\text{TmenCuAcac}(\text{ClO}_4)]$ (III) (Acac representing acetylacetonato). All the data are converging to show that two antiferromagnetic interactions are operative in solid samples of I. Surprisingly, the larger interaction ($|J|$ = 1.0 cm^{-1}) is found to be intermolecular in nature whereas the intramolecular interaction is significantly smaller ($|J'|$ = 0.08 cm^{-1}). As for II and III, one antiferromagnetic interaction is operative in each case. However, the interaction is intramolecular for II and, obviously, intermolecular for the mononuclear complex III.

Introduction

The study of exchange-coupled polynuclear complexes is an active area of coordination chemistry.[1] In many instances, a close dependence of the isotropic exchange parameter (J) on some structural factor has been demonstrated and understood on the basis of the orbital mechanism of exchange interaction.[2]

Among the various topics which are presently under study and, therefore, not completely elucidated, a great interest is given to complexes exhibiting large exchange pathways generally associated with weak J values. In these cases, spectroscopic techniques such as optical spectroscopy,[3] inelastic electron scattering,[4] EPR,[5,6] etc. are very useful as complements to susceptibility measurements because they may offer a direct access to the singlet–triplet energy gap in dinuclear complexes and the origin (intra- or intermolecular) of the interaction.[5,7-10] The present paper affords a new example of this complementarity.

We have synthesized and characterized two formally dinuclear copper(II) complexes, $[(\text{TmenCu})_2\text{Tae}(\text{ClO}_4)_2{\cdot}\text{H}_2\text{O}]$ (I) and $[(\text{TmenCu})_2\text{Tae}{\cdot}\text{H}_2\text{O}[(\text{BPh}_4)_2$ (II), Tmen and Tae representing *N*,*N*,*N'*,*N'*-tetramethylenediamine and the dianion of tetraacetylethane, respectively. Their magnetic properties have been determined and compared to those of their mononuclear counterpart, $[\text{TmenCuAcac}(\text{ClO}_4)]$ (III), Acac being the anionic form of 2,4-pentanedione, to decipher the relative magnitudes of the intra and intermolecular interactions.

Mono- and dinuclear copper and nickel complexes of the Tae ligand were recently reported.[11-16] However, these studies were essentially devoted to thermochromic properties. They did not comprise any structural determination or detailed magnetic study. The structure of the free ligand H_2Tae has been solved via X-ray[17] and neutron[18] diffraction techniques.

Table I. Crystallographic Data for I[a]

chem formula $\text{Cu}_2\text{Cl}_2\text{O}_{13}\text{N}_4\text{C}_{22}\text{H}_{46}$	$F(000)$ = 1608
fw = 772.6	T = 20 ± 1 °C
space group: $P2_1/c$	λ = 0.710 73 Å
a = 15.598 (2) Å	ρ(calc) = 1.478 g cm^{-3}
b = 8.748 (1) Å	μ = 14.4 cm^{-1}
c = 26.508 (3) Å	transm coeff = 0.95–1.00
β = 106.22 (1)°	$R(F_o)$ = 0.024
V = 3473 (1) Å^3	R_w = 0.025
Z = 4	

[a] $R = \sum(|F_o| - |F_c|)/\sum|F_o|$. $R_w = [\sum w(|F_o| - |F_c|)^2/\sum w|F_o|^2]^{1/2}$.

Experimental Section

Materials. The ligand H_2Tae (tetraacetylethane) was synthesized by the method of Charles.[19] *N*,*N*,*N'*,*N'*-tetramethylethylenediamine (Tmen), 2,4-pentanedione (AcacH), and copper perchlorate hexahydrate, $\text{Cu}(\text{ClO}_4)_2{\cdot}6\text{H}_2\text{O}$ were purchased from Aldrich. The complexes $[(\text{TmenCuOH})_2[(\text{ClO}_4)_2$[20] and $[\text{TmenCuAcac}(\text{ClO}_4)]$ (Acac represents the anionic form of 2,4-pentanedione) were prepared by known procedures.

Solvents used for synthetic experiments and for spectroscopic measurements were of analytical grade available commercially.

Physical Measurements. Microanalyses were performed by the Service Central de Microanalyse du CNRS, Lyon, France. IR spectra were recorded on KBr disks with the help of a Perkin-Elmer 983 spec-

---

[1] *Magneto-Structural Correlations in Exchange Coupled Systems*; Willet, R. D., Gatteschi, D., Kahn, O., Eds.; D. Reidel: Dordrecht, The Netherlands, 1985.

[2] Kahn, O. *Struct. Bonding* **1987**, *68*, 89.

[3] See: Gudel, H. U. In ref 1, p 297 and references therein.

[4] See: Gudel, H. U. In ref 1, p 329 and references therein.

[5] Pierpont, C. G.; Francesconi, L. C.; Hendrickson, D. N. *Inorg. Chem.* **1977**, *16*, 2367.

[6] Duggan, D. M.; Hendrickson, D. N. *Inorg. Chem.* **1974**, *13*, 2929.

[7] Folgado, J. V.; Ibañez, R.; Coronado, E.; Beltran, D.; Savariault, J.-M.; Galy, J. *Inorg. Chem.* **1988**, *27*, 19.

[8] Francesconi, L. C.; Corbin, D. R.; Clauss, A. W.; Hendrickson, D. N. *Inorg. Chem.* **1981**, *20*, 2059.

[9] Hoffman, S. K.; Towle, D. K.; Hatfield, W. E.; Chaudhuri, P.; Wieghardt, K. *Inorg. Chem.* **1985**, *24*, 1307.

[10] Chiari, B.; Helms, J. H.; Piovesana, O.; Tarantelli, T.; Zannazzi, P. F. *Inorg. Chem.* **1986**, *25*, 870.

[11] Fukuda, Y.; Mafune, K. *Chem. Lett.* **1988**, 697.

[12] Fukuda, Y.; Sone, K. *Bull. Chem. Soc. Jpn.* **1972**, *45*, 465.

[13] Fukuda, Y.; Sone, K. *J. Inorg. Nucl. Chem.* **1972**, *34*, 2315.

[14] Fukuda, Y.; Shimura, A.; Mukaida, M.; Fujita, E.; Sone, K. *J. Inorg. Nucl. Chem.* **1974**, *36*, 1265.

[15] Sone, K.; Fukuda, Y. *Studies Phys. Theoret. Chem.* **1982**, *27*, 251.

[16] Fukuda, Y.; Kimura, H.; Sone, K. *Bull. Chem. Soc. Jpn.* **1982**, *55*, 3738.

[17] Schaefer, J.-P.; Wheatley, P. J. *J. Chem. Soc. A* **1966**, 528.

[18] Power, L. F.; Turner, K. E.; Moore, F. H. *J. Cryst. Mol. Struct.* **1975**, *5*, 59.

[19] Charles, R. G. *Org. Synth.* **1959**, *39*, 61.

[20] Meek, D. W.; Ehrhardt, S. A. *Inorg. Chem.* **1965**, *4*, 584.

0020-1669/92/1331-0284$03.00/0

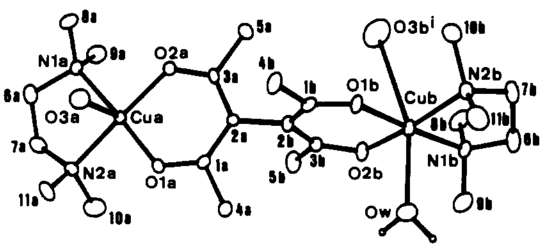

Figure 1. ORTEP plot of I with the numbering scheme. Hydrogen atoms are omitted for clarity. Symmetry operation: (Å) x, $1 + y$, z.

trometer, while electronic spectra were obtained with a Cary 2390 spectrophotometer. Magnetic susceptibility data were collected on powdered samples of the compounds with use of a Faraday-type magnetometer using mercury tetrakis(thiocyanato)cobaltate(III) (susceptibility at 20 °C 16.44×10^{-6} cm^3 mol^{-1}) as a susceptibility standard. Data were corrected for diamagnetism of the ligands and anions (estimated from the Pascal constants[21] to be -342×10^{-6} cm^3 mol^{-1} for I, -576×10^{-6} cm^3 mol^{-1} for II, and -178×10^{-6} cm^3 mol^{-1} for III) and eventually TIP (taken as 60×10^{-6} cm^3 mol^{-1}/Cu atom).

Magnetic susceptibility measurements of complexes in solution were determined by NMR[22] spectroscopy using dichloromethane as solvent and TMS as indicator with a Brucker WH 90 instrument.

Preparation of the Complexes. (Tetraacetylethanato(2−))bis((*N*,*N*,*N*′,*N*′-tetramethylethylenediamine)copper(II)) Diperchlorate Hydrate, [$(TmenCu)_2Tae(ClO_4)_2 \cdot H_2O$]. A dichloromethane solution (20 mL) of tetraacetylethane (0.67 g, 3.4 mM) was added to a dichloromethane solution (50 mL) of [$TmenCuOH]_2(ClO_4)_2$ (2 g, 3.4 mM). The resulting solution was stirred, heated under reflux for 15 min, and then filtered. The solution, left to stand overnight, afforded a purple precipitate, which was filtered out and dried as a powder. Yield: 75%. Anal. Calcd for $C_{22}H_{46}Cl_2Cu_2N_4O_{13}$: C, 34.2; H, 6.0; N, 7.3. Found: C, 34.4; H, 5.9; N, 7.4. Slow evaporation of a dichloromethane solution of this product in a diethyl oxide atmosphere gave crystals suitable for X-ray diffraction. Visible: λ_{max} in CH_2Cl_2 550 nm.

(Tetraacetylethanato(2−))bis((*N*,*N*,*N*′,*N*′-tetramethylethylenediamine)copper(II)) Bis(tetraphenylborate) Hydrate, [$(TmenCu)_2Tae \cdot H_2O](BPh_4)_2$. A 0.3-g sample of the above mentioned complex was dissolved in 15 mL of MeOH. The addition of a methanolic solution (10 mL) of $NaBPh_4$ (0.27 g, 7.8 mM) upon stirring induced an immediate brown precipitate, which was filtered and dried. Yield: 95%. Anal. Calcd for $C_{70}H_{86}B_2Cu_2N_4O_4$: C, 69.4; H, 7.1; N, 4.6. Found: C, 67.9; H, 7.0; N, 4.5. Visible: λ_{max} in CH_2Cl_2 550 nm.

Caution! As some of the complexes reported here were isolated as perchlorate salts, extreme caution should be taken in their handling due to their unforeseeable behavior.[23]

Crystallography. Crystallographic data are listed in Table I. A parallelepipedic dark blue crystal of dimensions 0.40 × 0.10 × 0.05 mm was glued on a glass fiber and mounted on an Enraf-Nonius CAD 4 diffractometer with graphite-monochromatized Mo Kα radiation. The unit cell was refined by using 25 reflections in the 2θ range 16–24°. A data set of 6343 reflections ($2 < \theta < 50°$; $h,k,\pm l$) was recorded as described previously[24] by the $\omega/2\theta$ scan technique (scan width 0.60° + 0.35° tan θ; scan speed 1.0–5.5°/min). The intensities of three standard reflections monitored every 2 h showed no noticeable change. Data reflections were corrected for LP[25] and for empirical absorption.[26] From the 6115 independent reflections ($0kl$ and $0k\bar{l}$ merged, $R_{av} = 0.018$), 3114 with $F_o^2 > 3\sigma(F_o^2)$ were retained and used for the structure solution and least-squares refinement.

The structure was solved by direct methods using SHELXS-86.[27] The atomic scattering factors used were those from Cromer and Waber[28] for non-hydrogen atoms and from Stewart et al.[29] for hydrogen one's.

Table II. Fractional Atomic Coordinates and Isotropic or Equivalent Temperature Factors (Å^2 × 100) with ESD's in Parentheses for I ($U_{eq} = {}^1/_3$(Trace $\tilde{U}$)

atom	x/a	y/b	z/c	U_{eq}/U_{iso}
Cu_a	0.74854 (3)	0.69300 (5)	0.71834 (2)	3.42 (7)
O_{1a}	0.6754 (2)	0.5480 (3)	0.6736 (1)	4.2 (5)
C_{1a}	0.5999 (2)	0.5743 (4)	0.6395 (2)	3.9 (7)
C_{2a}	0.5573 (2)	0.7153 (4)	0.6298 (1)	2.9 (6)
C_{3a}	0.5964 (2)	0.8471 (4)	0.6539 (2)	3.5 (7)
C_{4a}	0.5595 (3)	0.4345 (5)	0.6088 (2)	5.9 (9)
C_{5a}	0.5485 (3)	0.9978 (5)	0.6430 (2)	5.7 (9)
O_{2a}	0.6744 (2)	0.8573 (3)	0.6866 (1)	4.4 (5)
N_{1a}	0.8353 (2)	0.8404 (3)	0.7655 (1)	3.3 (5)
C_{6a}	0.9110 (3)	0.7422 (6)	0.7955 (2)	5.7 (8)
C_{7a}	0.8790 (3)	0.5966 (5)	0.8094 (2)	5.9 (9)
N_{2a}	0.8167 (2)	0.5225 (4)	0.7646 (1)	3.7 (6)
C_{8a}	0.8683 (3)	0.9555 (5)	0.7349 (2)	5.3 (9)
C_{9a}	0.7921 (3)	0.9195 (5)	0.7999 (2)	6.0 (9)
C_{10a}	0.7567 (4)	0.4245 (6)	0.7845 (2)	8 (1)
C_{11a}	0.8633 (3)	0.4272 (5)	0.7354 (2)	5.6 (9)
Cu_b	0.26220 (3)	0.74986 (6)	0.51484 (2)	3.49 (7)
O_{1b}	0.3777 (1)	0.7732 (3)	0.50494 (9)	3.8 (4)
C_{1b}	0.4529 (2)	0.7594 (4)	0.5392 (1)	3.7 (6)
C_{2b}	0.4640 (2)	0.7219 (4)	0.5923 (1)	3.4 (6)
C_{3b}	0.3919 (2)	0.6927 (4)	0.6128 (1)	3.4 (6)
C_{4b}	0.5333 (2)	0.7815 (5)	0.5195 (2)	5.2 (8)
C_{5b}	0.4067 (3)	0.6518 (6)	0.6692 (2)	7 (1)
O_{2b}	0.3097 (2)	0.6888 (3)	0.5859 (1)	4.5 (5)
N_{1b}	0.1366 (2)	0.7332 (4)	0.5232 (1)	3.9 (5)
C_{6b}	0.0752 (2)	0.7630 (6)	0.4715 (2)	6.3 (9)
C_{7b}	0.1100 (3)	0.8807 (6)	0.4437 (2)	7 (1)
N_{2b}	0.2032 (2)	0.8493 (4)	0.4439 (1)	4.0 (6)
C_{8b}	0.1259 (3)	0.8444 (5)	0.5627 (2)	7 (1)
C_{9b}	0.1171 (3)	0.5799 (5)	0.5399 (2)	7 (1)
C_{10b}	0.2486 (3)	0.9929 (5)	0.4368 (2)	7 (1)
C_{11b}	0.2066 (3)	0.7502 (6)	0.4006 (2)	7 (1)
O_w	0.2701 (2)	0.4838 (4)	0.4825 (1)	6.6 (7)
H_1O_w	0.294 (3)	0.428 (3)	0.5149 (8)	7.0
H_2O_w	0.230 (2)	0.415 (3)	0.458 (1)	7.0
Cl_a	0.92610 (6)	0.6761 (1)	0.62643 (4)	4.3 (2)
O_{3a}	0.8466 (2)	0.6779 (4)	0.6422 (1)	7.5 (7)
O_{4a}	0.9806 (3)	0.7933 (6)	0.6493 (2)	14 (1)
O_{5a}	0.9685 (3)	0.5361 (5)	0.6373 (2)	12 (1)
O_{6a}	0.9036 (2)	0.6921 (5)	0.5721 (1)	8.9 (8)
Cl_b	0.30144 (7)	0.1849 (1)	0.59120 (5)	5.8 (2)
O_{3b}	0.3149 (3)	0.0451 (5)	0.5717 (3)	15 (1)
O_{4b}	0.2103 (2)	0.2166 (4)	0.5792 (2)	9.4 (8)
O_{5b}	0.3458 (3)	0.2926 (6)	0.5719 (2)	14 (1)
O_{6b}	0.3366 (3)	0.1780 (7)	0.6444 (2)	16 (1)

Completion and refinement of the structure were carried out by difference electron density maps and least-squares refinement processes using SHELX-76.[30] All non-hydrogen atoms were refined anisotropically. All hydrogen atoms but those of the water molecule were introduced in constrained geometry (C–H = 0.97 Å). Water molecule H's were allowed to vary. A general isotropic temperature factor for H atoms was first refined and then kept fixed to 0.07 Å^2. The refinement converged to $R = 0.024$ and $R_w = 0.025$ (Table I) with 394 variable parameters and with a maximum shift/esd of 0.11 (a H parameter), the mean shift/esd being equal to 0.008, on the final full-matrix least-squares refinement cycle and a maximum peak of 0.3 e/Å^3. The atomic coordinates are listed in Table II.

Results and Discussion

Description of the Structure of [$(TmenCu)_2Tae(ClO_4)_2 \cdot H_2O$]. Figure 1 is a view of the binuclear unit with the atom-numbering scheme indicated. Interatomic bond distances and angles are listed in Table III.

In the binuclear unit, the two copper ions are not equivalent, since one Cu_a is in a (4 + 1) surrounding while the other Cu_b seemingly adopts a (4 + 1 + 1) coordination. In both cases however, the four nearest neighbors, at about 2 Å, are two oxygen atoms, O_{1x} and O_{2x} (x = a, b), from Tae and two nitrogen atoms,

---

(21) Pascal, P. *Ann. Chim. Phys.* **1910**, *19*, 5.

(22) Evans, D. F. *Proc. Chem. Soc.* **1958**, 115.

(23) Everett, K.; Graf, F. A., Jr. *CRC Handbook of Laboratory Safety*, 2nd ed.; Steere, N. V., Ed.; Chemical Rubber Co.: Cleveland, OH, 1971.

(24) Mosset, A.; Bonnet, J.-J.; Galy, J. *Acta Crystallogr., Sect. B* **1977**, *B33*, 2639.

(25) B. A. Frenz, & Associates, Inc. *SDP-Structure Determination Package*; College Station, TX 77840, and Enraf-Nonius, Delft, Holland, 1985.

(26) North, A. C. T.; Phillips, D. C.; Mathews, F. S. *Acta Crystallogr., Sect. A* **1968**, *A24*, 351.

(27) Sheldrick, G. M. *SHELXS86, Program for Crystal Structure Solution*; University of Göttingen: Göttingen, FRG, 1986.

(28) Cromer, D. T.; Waber, J. T. *International Tables for X-ray Crystallography*; Ibers, J. A., Hamilton, W. C., Eds.; Kynoch Press: Birmingham, England, 1974; Vol. IV, Table 2.2.B, p 99 and Table 2.3.1, p 149.

(29) Stewart, R. F.; Davidson, E. R.; Simpson, W. T. *J. Chem. Phys.* **1965**, *42*, 3175.

(30) Sheldrick, G. M. *SHELX76, Program for Crystal Structure Determination*; University of Cambridge: Cambridge, England, 1976.

Table III. Bond Lengths (Å) and Angles (deg) for I with Estimated Standard Deviations in Parentheses[a]

Cu_a-O_{1a}	1.887 (2)	Cu_b-O_{1b}	1.903 (2)
Cu_a-O_{2a}	1.889 (2)	Cu_b-O_{2b}	1.897 (3)
Cu_a-N_{1a}	2.027 (3)	Cu_b-N_{1b}	2.038 (3)
Cu_a-N_{2a}	2.032 (3)	Cu_b-N_{2b}	2.042 (3)
Cu_a-O_{3a}	2.855 (4)	Cu_b-O_w	2.496 (3)
		$Cu_b-O_{3b}{}^i$	2.988 (5)
$O_{1a}-Cu_a-O_{2a}$	92.5 (1)	$O_{1b}-Cu_b-O_{2b}$	92.6 (1)
$O_{1a}-Cu_l-N_{1a}$	175.6 (1)	$O_{1b}-Cu_b-N_{1b}$	177.4 (1)
$O_{1a}-Cu_a-N_{2a}$	90.5 (1)	$O_{1b}-Cu_b-N_{2b}$	91.6 (1)
$O_{2a}-Cu_a-N_{1a}$	90.6 (1)	$O_{2b}-Cu_b-N_{1b}$	89.6 (1)
$O_{2a}-Cu_a-N_{2a}$	168.3 (1)	$O_{2b}-Cu_b-N_{2b}$	169.8 (1)
$N_{1a}-Cu_a-N_{2a}$	87.0 (1)	$N_{1b}-Cu_b-N_{2b}$	86.0 (1)
$O_{3a}-Cu_a-Cu_{1a}$	87.7 (1)	$O_w-Cu_b-O_{1b}$	85.0 (1)
$O_{3a}-Cu_a-O_{2a}$	95.9 (1)	$O_w-Cu_b-O_{2b}$	92.0 (1)
$O_{3a}-Cu_a-N_{1a}$	93.9 (1)	$O_w-Cu_b-N_{1b}$	96.4 (1)
$O_{3a}-Cu_a-N_{2a}$	95.7 (1)	$O_w-Cu_b-N_{2b}$	97.7 (1)
		$O_{3b}{}^i-Cu_b-O_{1b}$	80.7 (1)
		$O_{3b}{}^i-Cu_b-O_{2b}$	76.5 (1)
		$O_{3b}{}^i-Cu_b-N_{1b}$	98.3 (1)
		$O_{3b}{}^i-Cu_b-N_{2b}$	95.0 (1)
		$O_{3b}{}^i-Cu_b-O_w$	161.2 (1)
$O_{1a}-C_{1a}$	1.290 (4)	$O_{1b}-C_{1b}$	1.272 (4)
$C_{1a}-C_{2a}$	1.391 (5)	$C_{1b}-C_{2b}$	1.407 (5)
$C_{1a}-C_{4a}$	1.506 (6)	$C_{1b}-C_{4b}$	1.501 (6)
	$C_{2a}-C_{2b}$	1.517 (4)	
$C_{2a}-C_{3a}$	1.375 (5)	$C_{2b}-C_{3b}$	1.404 (5)
$C_{3a}-O_{2a}$	1.284 (4)	$C_{3b}-O_{2b}$	1.282 (4)
$C_{3a}-C_{5a}$	1.503 (5)	$C_{3b}-C_{5b}$	1.490 (6)
$N_{1a}-C_{6a}$	1.496 (5)	$N_{1b}-C_{6b}$	1.458 (5)
$N_{1a}-C_{8a}$	1.473 (6)	$N_{1b}-C_{8b}$	1.474 (6)
$N_{1a}-C_{9a}$	1.453 (6)	$N_{1b}-C_{9b}$	1.470 (6)
$C_{6a}-C_{7a}$	1.453 (7)	$C_{6b}-C_{7b}$	1.456 (7)
$N_{2a}-C_{7a}$	1.459 (5)	$N_{2b}-C_{7b}$	1.480 (5)
$N_{2a}-C_{10a}$	1.471 (7)	$N_{2b}-C_{10b}$	1.480 (6)
$N_{2a}-C_{11a}$	1.463 (6)	$N_{2b}-C_{11b}$	1.450 (6)
$Cu_a-O_{1a}-C_{1a}$	126.5 (2)	$Cu_b-O_{1b}-C_{1b}$	127.6 (3)
$O_{1a}-C_{1a}-C_{2a}$	125.6 (3)	$O_{1b}-C_{1b}-C_{2b}$	124.6 (3)
$O_{1a}-C_{1a}-C_{4a}$	113.4 (3)	$O_{1b}-C_{1b}-C_{4b}$	115.6 (3)
$C_{2a}-C_{1a}-C_{4a}$	121.0 (3)	$C_{2b}-C_{1b}-C_{4b}$	119.7 (3)
$C_{1a}-C_{2a}-C_{3a}$	122.1 (3)	$C_{1b}-C_{2b}-C_{3b}$	122.8 (3)
$C_{1a}-C_{2a}-C_{2b}$	118.4 (3)	$C_{1b}-C_{2b}-C_{2a}$	119.5 (3)
$C_{3a}-C_{2a}-C_{2b}$	119.5 (3)	$C_{3b}-C_{2b}-C_{2a}$	117.7 (3)
$C_{2a}-C_{3a}-O_{2a}$	125.8 (3)	$C_{2b}-C_{3b}-O_{2b}$	125.0 (3)
$C_{2a}-C_{3a}-C_{5a}$	120.9 (3)	$C_{2b}-C_{3b}-C_{5b}$	121.0 (3)
$O_{2a}-C_{3a}-C_{5a}$	113.3 (3)	$O_{2b}-C_{3b}-C_{5b}$	113.8 (3)
$Cu_a-O_{2a}-C_{3a}$	126.5 (2)	$Cu_b-O_{2b}-C_{3b}$	126.7 (3)
$Gu_a-N_{1a}-C_{6a}$	104.7 (2)	$Cu_b-N_{1b}-C_{6b}$	106.5 (2)
$Cu_a-N_{1a}-C_{8a}$	111.8 (2)	$Cu_b-N_{1b}-C_{8b}$	109.5 (2)
$Cu_a-N_{1a}-C_{9a}$	110.1 (2)	$Cu_b-N_{1b}-C_{9b}$	112.6 (3)
$C_{6a}-N_{1a}-C_{8a}$	109.8 (3)	$C_{6b}-N_{1b}-C_{8b}$	112.0 (3)
$C_{6a}-N_{1a}-C_{9a}$	112.0 (3)	$C_{6b}-N_{1b}-C_{9b}$	108.0 (3)
$C_{8a}-N_{1a}-C_{9a}$	108.4 (3)	$C_{8b}-N_{1b}-C_{9b}$	108.3 (3)
$N_{1a}-C_{6a}-C_{7a}$	111.2 (3)	$N_{1b}-C_{6b}-C_{7b}$	111.2 (3)
$C_{6a}-C_{7a}-N_{2a}$	112.4 (4)	$C_{6b}-C_{7b}-N_{2b}$	111.8 (4)
$Cu_a-N_{2a}-C_{7a}$	106.4 (2)	$Cu_b-N_{2b}-C_{7b}$	105.8 (3)
$Cu_a-N_{2a}-C_{10a}$	111.5 (3)	$Cu_b-N_{2b}-C_{10b}$	111.7 (2)
$Cu_a-N_{2a}-C_{11a}$	110.6 (3)	$Cu_b-N_{2b}-C_{11b}$	111.6 (3)
$C_{7a}-N_{2a}-C_{10a}$	108.3 (4)	$C_{7b}-N_{2b}-C_{10b}$	110.3 (3)
$C_{7a}-N_{2a}-C_{11a}$	111.5 (3)	$C_{7b}-N_{2b}-C_{11b}$	111.2 (3)
$C_{10a}-N_{2a}-C_{11a}$	108.5 (3)	$C_{10b}-N_{2b}-C_{11b}$	106.4 (4)
Cl_a-O_{3a}	1.416 (4)	Cl_b-O_{3b}	1.367 (5)
Cl_a-O_{4a}	1.362 (5)	Cl_b-O_{4b}	1.395 (4)
Cl_a-O_{5a}	1.383 (4)	Cl_b-O_{5b}	1.351 (5)
Cl_a-O_{6a}	1.390 (3)	Cl_b-O_{6b}	1.364 (4)
$O_{3a}-Cl_a-O_{4a}$	110.5 (3)	$O_{3b}-Cl_b-O_{4b}$	110.3 (3)
$O_{3a}-Cl_a-O_{5a}$	110.8 (3)	$O_{3b}-Cl_b-O_{5b}$	109.4 (4)
$O_{3a}-Cl_a-O_{6a}$	108.4 (2)	$O_{3b}-Cl_b-O_{6b}$	106.9 (4)
$O_{4a}-Cl_a-O_{5a}$	111.8 (3)	$O_{4b}-Cl_b-O_{5b}$	111.8 (3)
$O_{4a}-Cl_a-O_{6a}$	109.3 (3)	$O_{4b}-Cl_b-O_{6b}$	109.5 (3)
$O_{5a}-Cl_a-O_{6a}$	105.8 (3)	$O_{5b}-Cl_b-O_{6b}$	108.8 (3)
$O_w-H_1O_w$	0.97 (2)	$O_w-H_2O_w$	0.97 (3)
	$H_1O_w-O_w-H_2O_w$	107 (2)	
$Cu_b-O_w-H_1O_w$	102 (2)	$Cu_b-O_w-H_2O_w$	136 (2)
$O_w-H_1O_w\cdots O_{5b}$	171 (3)	$O_w-H_2O_w\cdots O_{6a}{}^{ii}$	151 (3)
$O_w\cdots O_{5b}$	2.872 (6)	$O_w\cdots O_{6a}{}^{ii}$	3.100 (5)
$H_1O_w\cdots O_{5b}$	1.91 (2)	$H_2O_w\cdots O_{6a}{}^{ii}$	2.22 (3)

[a] Symmetry operations: (i) $x, 1 + y, z$; (ii) $1 - x, 1 - y, 1 - z$.

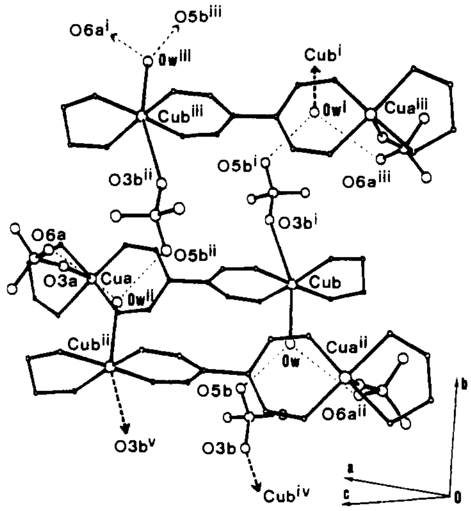

Figure 2. Molecular packing with a schematic representation of hydrogen bonds. The methyl groups of Tae and Tmen are omitted for clarity. Symmetry operations: (i) $x, 1 + y, z$; (ii) $1 - x, 1 - y, 1 - z$; (iii) $1 - x, 2 - y, 1 - z$; (iv) $x, -1 + y, z$; (v) $1 - x, -y, 1 - z$.

N_{1x} and N_{2x}, from Tmen. The apical position of Cu_a is occupied by an oxygen atom O_{3a} from a perchlorate anion, at a distance of 2.855 (4) Å. As for Cu_b, the apical positions are occupied by two oxygen atoms belonging to a water molecule O_w and a perchlorate anion $O_{3b}{}^i$ from an adjacent unit. The related distances are $Cu_b\cdots O_w$ = 2.496 (3) Å and $Cu_b\cdots O_{3b}{}^i$ = 2.988 (5) Å. It may be noted that the two $Cu_x\cdots O(ClO_4)$ distances are large, so that the perchlorate anions can be considered as semicoordinated at the best.

In each moiety, the equatorial donors, N_{1x}, N_{2x}, O_{1x}, and O_{2x}, lie approximately in a plane, the maximum deviations from planarity being 0.163 (3) Å for x = a and 0.083 (3) Å for x = b. The copper ions are not far removed from these mean planes. The deviations of 0.0608 (5) Å for Cu_a and 0.0873 (5) Å for Cu_b are much lower than the values (0.2–0.3 Å) generally reported for copper atoms involved in (4 + 1) coordination.[31] The dihedral angle between the two mean coordination planes is 77.0°, and the $Cu_a\cdots Cu_b$ separation through the Tae ligand is 8.0020 (6) Å.

The two acetylacetonato moieties are planar, the maximum deviation from planarity being 0.044 (4) Å. The two related mean planes make an angle of 82.5°, while an angle of 87.6° is reported for the free ligand.[18] With a value of 1.517 (4) Å, the C–C bond which links the two acetylacetonato residues is slightly larger than in the uncomplexed ligand, where the reported value is 1.486 (3) Å. This C–C bond must be considered as simple.

The binuclear units are packed along the *b* direction, and they are linked via water molecules and perchlorate anions (Figure 2). However, two binding modes have to be considered. In both cases the oxygen atom of a water molecule, axially coordinated to a Cu_b ion, is hydrogen-bonded to an oxygen atom which may belong either to a perchlorate group semicoordinated to Cu_a of an adjacent unit or to a perchlorate group semicoordinated to Cu_b of a next-neighbor unit. In the former case the resulting structure would consist of isolated "dimers of a dimer". Within each tetranuclear entity, the interdimer $Cu_a\cdots Cu_b$ separation of 7.2571 (7) Å is shorter than the intradimer $Cu_a\cdots Cu_b$ separation of 8.0020 (6) Å. The second possibility would yield an "alternate ladderlike" structure with a $Cu_b\cdots Cu_b$ separation of 8.7480 (7) Å. Indeed, in this structure, the Cu_a ions are not involved in the bridging framework.

Magnetic Susceptibility Measurements. Variable-temperature susceptibility data have been collected down to 4.5 K for the three complexes.

In the case of I, a plot of χ^{-1} vs T is linear in the temperature range 300 < T < 50 K with a negative temperature intercept of

---

[31] Maroney, M. J.; Rose, N. J. *Inorg. Chem.* **1984**, *23*, 2252 and references therein.

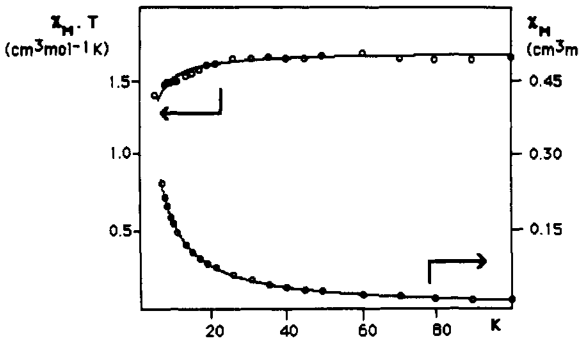

Figure 3. Experimental (○) and calculated temperature dependences of $\chi_M T$ and χ_M for I. The calculated curves correspond to a "dimer of a dimer" model (see text).

$\Theta = -4.44$ K and a Curie constant of 0.43 cm^3 atom^{-1} K. In the high-temperature range, I can be considered as slightly antiferromagnetic. At low temperatures, feable deviations from the Curie–Weiss behavior are observed, suggesting the occurrence of a second interaction whose magnitude would be much smaller than that of the first one.

As for II, the temperature dependence of its susceptibility is well described by the Curie law $C = 0.41$ cm^3 atom^{-1} K in the whole temperature range. The absence of any indication of an exchange interaction in susceptibility measurements taken down to 4.5 K means that $|J| < 0.4$ cm^{-1}.

Interestingly, the temperature variation of the susceptibility of III is according to the Curie–Weiss law ($C = 0.44$ cm^3 atom^{-1} K, $\Theta = -6.43$ K) in the range 300–4.5 K.[32] In this case the antiferromagnetic interaction gauged by the Θ value are obviously intermolecular in nature.

Finally, this rough analysis of the magnetic data obtained for I–III suggests that, in I and III, intermolecular couplings are operative. They would be supplemented by intramolecular interactions of feebler magnitudes in the case of I.

At this point of the discussion, the problem at hand is the choice of a suitable model for analyzing further the magnetic behavior of I. From the structural data, there are two possibilities. Indeed we can consider either a "dimer of a dimer" or an "alternate" ladderlike chain of dimers (Figure 2).

As we suspect that one interaction is larger than the other(s), an attempt is initially made to fit the data of a dimer model through the use of the Bleaney–Bower relation.[33] The best fit obtained in this manner yields $J = -2.5$ cm^{-1}, $g = 2.11$, and $R = 6.5 \times 10^{-3}$. Then to improve the quality of the model we consider an idealized tetranuclear (dimer of a dimer) structure involving two exchange parameters.[33] From the fit of the experimental data to the expression

$$\chi_m = \frac{N_g{}^2\beta^2}{3kT} \times \frac{30e^{A/kT} + 6e^{B/kT} + 6e^{-B/kT} + 6e^{-A/kT}}{5e^{A/kT} + 3e^{B/kT} + 3e^{-B/kT} + 3e^{-A/kT} + e^{-(A-2F)/kT} + e^{-(A+2F)/kT}}$$

with $A = J + J'$, $B = J - J'$, and $F = (J^2 + J'^2 - JJ')^{1/2}$, we obtain $J = -1.0$ cm^{-1}, $J' = -0.1$ cm^{-1}, $g = 2.09$, and R $= 2.3 \times 10^{-4}$ (Figure 3). It may be noted that slight variations of J' ($\Delta J' = \pm 0.04$ cm^{-1}) do not affect the quality of the fit.

As for the second structural possibility, we are faced with important difficulties which have been stressed by many authors.[10,35–41] Finally, we retained the Heisenberg model for isotropic coupling, which, according to Jotham,[42] gives a good description of the behavior of antiferromagnetically coupled chain compounds. Since this model cannot be solved accurately now, we have to use polynomial expressions such as that derived by Jotham[42] to obtain

$$J = -0.7 \text{ cm}^{-1} \qquad g = 2.11 \qquad R = 1.2 \times 10^{-3}$$

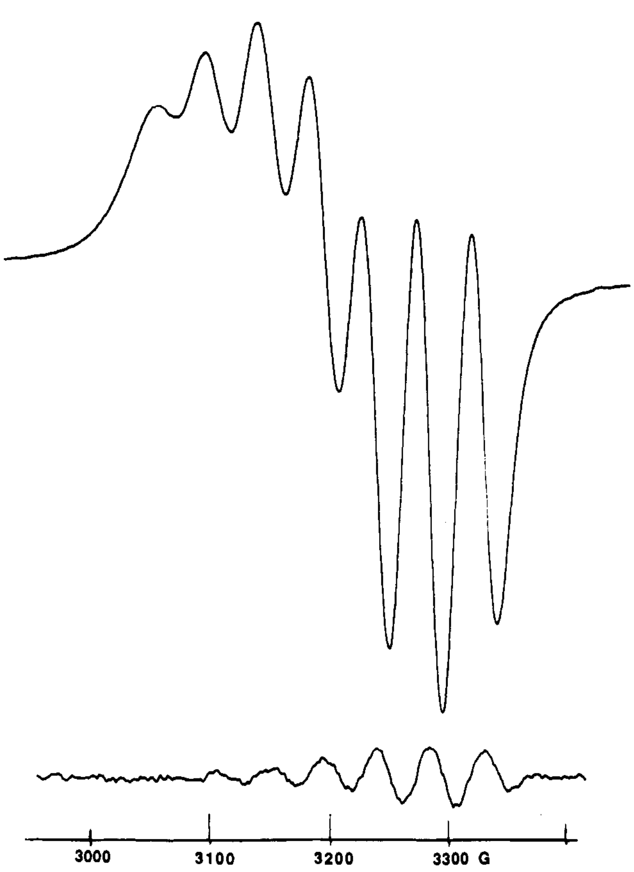

Figure 4. Isotropic ESR spectrum of I in solution (CH_2Cl_2, $T = 295$ K, X-band) with its second derivative.

The best description of the magnetic behavior of I is likely given by the tetranuclear (or dimer of a dimer) model with two exchange parameters differing by 1 order of magnitude.

ESR Spectroscopy. At room temperature, the X-band powder spectrum of I comprises two features peaking at $g \sim 2.13$ and $g \sim 2.06$, with widths of 93 and 36 G, respectively. For II, we observe a broad (240 G) derivative-like resonance centered at g ~ 2.07. "Bumps" of very low intensity are discernible on the low-field portion of the main signal. Lowering the temperature to 4.5 K does not modify the overall appearance of these spectra. However, raising the gain of the spectrometer allows the observation of new signals in both spectra. Two of these features appear at lower field of the $\Delta M_s = 1$ transition, while the third one is located at higher field. From their resonance field positions, one signal ($g \sim 4.1$) is assigned as the forbidden $\Delta M_s = 2$ transition. The other two signals, which, in both complexes, are equally distant from the $\Delta M_s = 1$ feature, are likely attributable to forbidden transitions involving the singlet electronic state of an exchange-coupled dimer and the $M_s = \pm 1$ components of the related triplet state.

The importance of observing the singlet–triplet transitions[5–7] arises from the fact that the absolute value of the corresponding exchange parameter $|J|$ can be determined from their magnetic

---

(32) Costes, J.-P.; Laurent, J.-P. Unpublished results.

(33) Bleaney, B.; Bowers, K. D. *Proc. R. Soc. London, Ser. A.* **1952**, *214*, 451.

(34) Jotham, R. W.; Kettle, S. F. A. *Inorg. Chim. Acta* **1970**, *4*, 145.

(35) Estes, W. E.; Hatfield, W. E.; van Ooijen, J. A. C.; Reedijk, J. *J. Chem. Soc., Dalton Trans.* **1980**, 2121.

(36) van Ooijen, J. A. C.; Reedijk, J. *J. Chem. Soc., Dalton Trans.* **1978**, 1170.

(37) Hall, J. W.; Marsh, W. E.; Weller, R. R.; Hatfield, W. E. *Inorg. Chem.* **1981**, *20*, 1033.

(38) Swank, D. D.; Willet, R. D. *Inorg. Chem.* **1980**, *19*, 2321.

(39) Chiari, B.; Helms, J. H.; Piovesana, O.; Tarantelli, T.; Zanazzi, P. F. *Inorg. Chem.* **1986**, *25*, 2408.

(40) Julve, M.; Verdaguer, M.; Faus, J.; Tinti, F.; Moratal, J.; Monge, A.; Gutierrez-Puebla, E. *Inorg. Chem.* **1987**, *26*, 3520.

(41) Gerstein, B. C.; Gehring, F. O.; Willett, R. D. *J. Appl. Phys.* **1972**, *43*, 1932.

(42) Jotham, R. W. *J. Chem. Soc., Dalton Trans.* **1977**, 266.

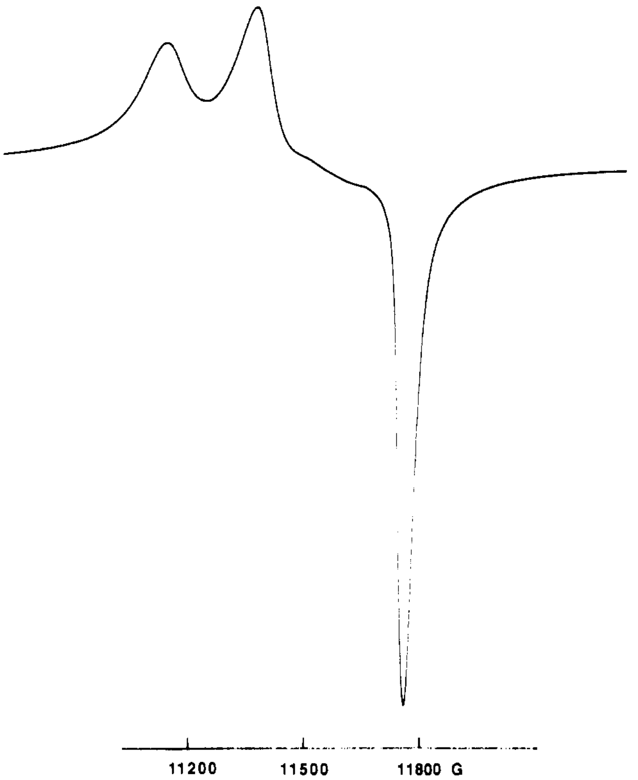

Figure 5. Q-band ESR spectrum of I as a powder (T = 295 K).

field positions. Indeed each of these transitions is expected to be at an energy of $2|J'|/g\beta$ to either higher or lower field of the $\Delta M_s = 1$ transition. When such information is applied to the spectra of I and II, this gives $|J'|$ = 0.08 cm^{-1} (I) and 0.05 cm^{-1} (II). It may be noted that this analysis is fully consistent with the "dimer of a dimer" model used for the susceptibility data. Taken together, both sets of results agree with the occurrence of two antiferromagnetic interactions: one would be intermolecular in nature and characterized by $-J$ = 1.0 cm^{-1}, while the other would be intramolecular and characterized by $-J' \sim 0.1$ cm^{-1}. This conclusion is further supported by a closer examination of the ESR data.

The room-temperature solution spectra[43] of I and II, which are expected to be mainly affected by intramolecular processes, display surprising seven-line patterns (Figure 4). This pattern is retained in various solvents, but the spacing between the lines and the related g_i values are solvent-dependent. For instance, in the case of I, $|A_i|$ varies from 48 G (CH_2Cl_2) to 38 G (i-$C_3H_7NH_2$) and g_i from 2.10_5 to 2.13. The usual four-line spectrum ($|A_i|$ = 88 G, $g_i = 2.10_5$) is observed for III (CH_2Cl_2 solution). It is known[5,44] that the room-temperature spectrum of an exchange-coupled (J') dinuclear complex looks like that of its mononuclear counterpart only if $|J'| \ll |A_i|$, A_i being the isotropic value of the hyperfine constant for the mononuclear species.

If $|J'| \gg |A_i|$, then the two unpaired electrons are exchanging rapidly on the ESR time scale between the two sites. The resulting isotropic spectrum for a dinuclear copper(II) complex displays seven hyperfine lines with a separation equal to $|A_i|/2$.[45] This is exactly what wer observe for complexes I and II, which therefore may display intramolecular interaction with coupling constants $|J'| \gg 0.009$ cm^{-1}. This condition is fulfilled by the aforementioned values of 0.08 cm^{-1} (I) and 0.05 cm^{-1} (II).

Let us now turn to the intermolecular interactions. One may expect to detect them in powder spectra. We have already reported the main features of the X-band spectra, which are uninformative as is the Q-band spectrum of II. On the contrary, the Q-band spectra of I and III display narrow ($\Delta H \leq 40$ G) and well-defined signals. The apparent g values [$g_1^{ex} = 2.17$, $g_2^{ex} = 2.13$, and $g_3^{ex} = 2.05$ for I (Figure 5) and $g_1^{ex} = 2.13_5$ and $g_2^{ex} = 2.06$ for III differ significantly from the values observed for dilute samples [$g_\parallel = 2.24_5$ and $g_\perp = 2.05$ for I and $g_\parallel = 2.21$ and $g_\perp = 2.05_5$ for III]. These discrepancies are likely attributable to exchange interactions between ESR spectroscopically nonequivalent sites. It is known[49] that for a solid sample such an interaction can induce a coupled **g** tensor whose components (g_i^{ex}) are related to the molecular values ($g_\parallel$ and $g_\perp$) by the following expressions:

$$g_1^{ex} = (\cos^2 \gamma)g_\parallel + (\sin^2 \gamma)g_\perp$$

$$g_2^{ex} = (\sin^2 \gamma)g_\parallel + (\cos^2 \gamma)g_\perp \qquad g_3^{ex} = g_\perp$$

Here 2γ is the canting angle between the normals to the equatorial planes of the two interacting ions. In addition, narrowing of the coupled signals may be observed.

We have noted previously that the widths of the signals are, for both complexes, relatively narrow. As for the g values, if we apply the aforementioned relations, we obtain

complex I: $2\gamma = 78.5°$; $g_\parallel = 2.25$, $g_\perp = 2.05$

complex III: $2\gamma = 90°$; $g_\parallel = 2.21$, $g_\perp = 2.06$

The resulting g values are almost identical to those observed for diluted samples and, therefore, may be considered as molecular g values. In the case of I, the 2γ value is in reasonable agreement with crystallographic data. Indeed, the normals to the equatorial planes around a Cu_a ion (x, y, z) and the Cu_b ion ($1 - x$, $1 - y$, $1 - z$) of an adjacent dinuclear unit (Figure 1) have been found to make an angle of 77.0°.

As for the Q band of II, the broadness ($\Delta H \sim 290$ G) may be attributed to dipolar interactions or/and a very weak exchange between equivalent ions.

Finally, a comparative analysis of the magnetic properties of the three complexes yields converging evidence of the following: (i) Complex I shows *intra-* and *inter*molecular antiferromagnetic interactions whereas intramolecular interactions alone are operative in complex II. Obviously, the interactions are intermolecular in the mononuclear complex III.

(ii) The intermolecular exchange interactions ($|J| \sim 1.0$ cm^{-1} for complexes I and III) are seemingly 1 order of magnitude larger than the intramolecular ones ($|J|$ = 0.08 cm^{-1} for I and 0.05 cm^{-1} for II). It may be noted that $|J|$ and $|J'|$ may be temperature dependent.[9] However, the resulting variations are expected to be small[9] enough not to alter the conclusion that $|J'| < |J|$.

The lack of intermolecular interactions in complex II has to be related to the fact that, unlike ClO_4, BPh_4 counterions are unable to semicoordinate to the copper ions and therefore to participate in a bridging network between dinuclear entities. Furthermore, these large ions promote an efficient insulation of the magnetic centers.

The weakness of the intramolecular interactions is not unexpected, since the geometry observed for complex I and assumed for complex II is unfavorable to transmit exchange coupling. Indeed, the planes of the magnetic orbitals which are of the $d_{x^2-y^2}$ type are not far removed from being orthogonal.[2] In addition, the intradimer Cu···Cu distance is large (8.0020 (6) Å).

As for the intermolecular interactions, we first note that they allow choosing between the two schemes of intermolecular linking which are conceivable from the structural data. The most likely structure is a "dimer of a dimer" with an interdimer pathway comprising a H_2O molecule, a hydrogen bond, and a ClO_4 group

---

(43) A detailed study of solution spectra for I–III and related mononuclear complexes will be reported elsewhere.

(44) Harty, E. F.; Wilson, L. J.; Hendrickson, D. N. *Inorg. Chem.* **1978**, *17*, 1834.

(45) Brière R.; Dupeyre, R. M.; Lemaire, H.; Morat, C.; Rassat, A.; Rey, P. *Bull. Soc. Chim. Fr.* **1966**, 3290.

(46) Mixed-valence Cu(II)–Cu(I) complexes could also give similar seven-line spectra.[47,48] So, we carried out magnetic moment measurements in solution using Evans' method to check what was the right assertion. I and II display moments of 2.5 μ_B in agreement with two copper(II) ions in the binuclear entity.

(47) Gagné, R. R.; Koval, C. A.; Smith, T. J.; Cimolino, M. C. *J. Am. Chem. Soc.* **1979**, *101*, 4571.

(48) Sigwart, C.; Hemmerich, P.; Spence, J. T. *Inorg. Chem.* **1968**, *7*, 2545.

(49) Henke, W.; Kremer, S.; Meinen, D. *Inorg. Chem.* **1983**, *22*, 2858.

Inorg. Chem. **1992**, *31*, 289-294 **289**

(Figure 2). Although the resulting interdimer Cu···Cu separation is actually smaller (7.2571 (7) Å) than the intradimer Cu···Cu distance (8.0020 (6) Å), the difference of effectiveness between the two exchange pathways (intermolecular vs intramolecular) is surprising. Furthermore, the interdimer bridge is from an axial position at one copper atom to another axial position at the second copper and it is well-known that, for copper ions assuming square-based configurations, the spin density along these axial direction is very low. As noted elsewhere,[50] more data are needed to rationalize the ability of the extended bridging network to support significant magnetic data.

Acknowledgment. We thank Dr. Mari for his contribution to the magnetic measurements.

Registry No. I, 137918-27-5; II, 137918-29-7; III, 86959-37-7; $[TmenCuOH]_2(ClO_4)_2$, 14266-63-8.

Supplementary Material Available: Tables SI-SIV, listing hydrogen atomic positional and thermal parameters, final anisotropic thermal parameters, bond lengths and angles, and least-squares planes equations for I (5 pages); a table of calculated and observed structure factor amplitudes for I (15 pages). Ordering information is given on any current masthead page.

---

(50) Colacio, E.; Costes, J.-P.; Kivekas, R.; Laurent, J.-P.; Ruiz, J.; Sundberg, M. *Inorg. Chem.* **1991**, *30*, 1475 and references therein.

Contribution from the School of Chemical Sciences and Beckman Institute,
University of Illinois, Urbana-Champaign, Urbana, Illinois 61801

A Molecular Mechanics Model of Ligand Effects. 2. Binding of Phosphines to $Cr(CO)_5$

Kevin J. Lee and Theodore L. Brown*

Received May 1, 1991

Molecular mechanics methods have been employed to compute the energy-minimized structures of a series of 19 trialkylphosphines and their complexes with $Cr(CO)_5$. The comprehensive computational package BIOGRAF was employed, using the MMP2 force field. The computed structure of $Cr(CO)_5PMe_3$ is in good agreement with the structural parameters determined by X-ray diffraction. The ligand–metal complex steric interaction is often manifested in a tilting of the ligand with respect to the Cr–P bond, especially in the most unsymmetrical ligands. The Cr–P distance increases with increasing value of ligand cone angle. For the largest ligands, $P(t\text{-}Bu)_2(i\text{-}Pr)$ and $P(t\text{-}Bu)_3$, the Cr–P distance is about 0.39 Å longer than expected from extrapolation of the data for smaller ligands, indicative that excessive steric repulsions prevent normal metal–ligand bond formation. Excepting the two longest distances, the variation in Cr–P distance with cone angle is roughly linear, with a dependence on cone angle more than twice as great as for the phosphite complexes, reported earlier. The total energy varies monotonically with increasing ligand cone angle. However, the only component of the total energy change that varies in a regular way is the bond energy term. As ligand steric requirement increases, increasing van der Waals repulsive interactions between ligand and complex are offset by variations in corresponding attractive terms. Thus, there is not a regular increase in the total van der Waals energy with increasing cone angle. The structure of $Cr(CO)_5PMe_3$ was determined by conventional crystallographic techniques with Mo Kα X-rays. At −75 °C, the crystals belong to monoclinic space group $P2_1/c$ with $a = 6.946$ (2) Å, $b = 11.622$ (3) Å, $c = 14.935$ (3) Å, $\beta = 103.16$ (2)°, $V = 1174$ (1) Å^3, and $Z = 4$.

In the first paper of this series, we described a molecular mechanics model for the interaction between phosphorus ligands and a metal center and its application to the interaction of a series of phosphites with $Cr(CO)_5$.[1] In this contribution, we describe the application of the model to interaction of a series of trialkylphosphines with $Cr(CO)_5$. Throughout the series, there is a substantial variation in steric requirement, as a result of branching at either α- or β-carbon positions.

There are no published structural data available for a trialkylphosphine complex of $Cr(CO)_5$. As a means of further testing the computational results, we have obtained the crystal structure of $Cr(CO)_5PMe_3$.

Methods

Computations were carried out using BIOGRAF, a comprehensive package of molecular modeling tools developed and marketed by Molecular Simulations, Inc., of Sunnyvale, CA. The force field model employed is MMP2.[2] The components of the energy terms in the calculations are described in detail in a previous paper.[1] Table I lists added or modified parameters, where these differ from the standard MMP2 set or those listed in the previous paper. The major difference from the set employed with the phosphites consists in a longer equilibrium Cr–P bond of 2.35 Å, as compared with 2.30 Å assumed for the phosphites. The methods employed for locating minimum-energy structures have been described.[1]

It has been assumed in the computations that complex formation causes an increase in the equilibrium C–P–C bond angle in the ligand, from 93° characteristic of the free ligand to 100° characteristic of the complexed ligand. This assumption is consistent with molecular orbital calculations[3] as well as with the observed structural data. It results in essentially the same computed variations in energies as when a constant equilibrium value of 93° is assumed.

Experimental Section

All manipulations were carried out under an argon atmosphere using standard Schlenk techniques. Reagent grade CH_2Cl_2 (Fischer) was distilled from P_2O_5 under N_2. The following chemicals were obtained from commercial sources and used as received: Me_3PAgI (Aldrich), $AgNO_3$ (Mallincrodt), and reagent grade hexane (Aldrich). $Et_4N[Cr(CO)_5Cl]$ was prepared as described in the literature.[4] Solution infrared spectra were recorded on a Perkin-Elmer 1710 FT-IR spectrometer using a 0.5 mm path length cell with KCl windows.

$Cr(CO)_5PMe_3$ was prepared by a modification of a published procedure.[5] $Et_4N[Cr(CO)_5Cl]$ (0.736 g, 2.06 mmol) and $AgNO_3$ (0.560 g, 3.30 mmol) were dissolved in 100 mL of CH_2Cl_2. The solution turned dark orange, and a white precipitate formed. After 10 min of stirring, a solution containing Me_3PAgI (0.643 g, 2.07 mmol) dissolved in 35 mL of CH_2Cl_2 was added via cannula. Additional white precipitate formed. After 10–15 min, the solvent was removed in vacuo, leaving a white residue which gradually turned gray. The gray residue was extracted with 100 mL of hexane, and the volume was reduced in vacuo to about 4 mL. Storage of this solution at −20 °C produced large colorless needles of $Cr(CO)_5PMe_3$. (ν_{CO}(hexane) 2063 w, 1951 m, 1939 vs cm^{-1}; lit.[5] 2064 w, 1952 m, 1941 vs cm^{-1}).

X-ray Crystal Structure Determination of $Cr(CO)_5PMe_3$

A colorless, transparent, prismatic crystal with well-developed faces was mounted to a thin glass fiber. Diffraction data were collected at −75 °C on an Enraf-Nonius CAD4 automated κ-axis diffractometer employing Mo Kα ($\lambda = 0.71071$ Å) radiation. The intensity data were

---

(1) Caffery, M. L.; Brown, T. L. *Inorg. Chem.* **1991**, *30*, 3907–3914.

(2) (a) Burkert, U.; Allinger, N. L. *Molecular Mechanics*; ACS Monograph 177; American Chemical Society: Washington, DC, 1982. (b) Sprague, J. T.; Tai, J. C.; Yuh, Y.; Allinger, N. L. *J. Comput. Chem.* **1987**, *8*, 581.

(3) Magnuson, E. *Aust. J. Chem.* **1985**, *38*, 23.

(4) Wovkulich, M. J.; Atwood, J. D. *Organometallics* **1982**, *1*, 1316.

(5) Connor, J. A.; Jones, E. M.; McEwen, G. K. *J. Organomet. Chem.* **1972**, *43*, 357.

0020-1669/92/1331-0289$03.00/0